

IEICE **TRANSACTIONS**

on Communications

VOL. E98-B NO. 7
JULY 2015

The usage of this PDF file must comply with the IEICE Provisions on Copyright.

The author(s) can distribute this PDF file for research and educational (nonprofit) purposes only.

Distribution by anyone other than the author(s) is prohibited.

A PUBLICATION OF THE COMMUNICATIONS SOCIETY



The Institute of Electronics, Information and Communication Engineers
Kikai-Shinko-Kaikan Bldg., 5-8, Shibakoen 3chome, Minato-ku, TOKYO, 105-0011 JAPAN

Combined MTL-Fullwave Statistical Approach for Fast Estimation of Radiated Immunity of Spacecraft Cable Assemblies Involving Multipair Bundles

Flavia GRASSI^{†a)}, Giordano SPADACINI^{†b)}, Nonmembers, Sergio A. PIGNARI^{†c)}, Member, and Filippo MARLIANI^{††d)}, Nonmember

SUMMARY In this work, a computationally-efficient modeling approach is developed to predict the electromagnetic noise induced in the terminal units of random bundles of twisted-wire pairs mounted onboard spacecraft. The proposed model combines the results of a preliminary full-wave simulation, aimed at evaluating the electromagnetic field inside the space vehicle's metallic body, with a stochastic model of a random bundle, based on multiconductor transmission line (MTL) theory. Model assessment versus measurement data obtained characterizing real wiring harness in a full-scale satellite mock-up demonstrates the large sensitivity (up to 40 decibels) of the induced noise levels to different bundle configurations, and corroborates the effectiveness of the proposed simplified modeling strategy for estimating the modal noise voltages induced in the terminal units.

key words: *intra-system radiated immunity, random TWP bundles, satellites, stochastic modeling*

1. Introduction

Achieving intra-system electromagnetic compatibility (EMC) of units and interconnecting cable assemblies in complex electromagnetic (EM) environments, such as those of embedded systems typically employed in the automotive, aircraft, and aerospace sectors, represents a challenging task for EMC engineers. As a matter of fact, several methods for pre-compliance verification based on (a) preliminary measurement in cost- and time-effective setups as well as (b) prediction by analytical and/or numerical models, are currently involved in the design flow and considered crucial check points to achieve EMC. In particular, simulation is nowadays considered a powerful tool (sometimes, in case of complex systems, it may even be a substitute for measurement), as it offers the additional advantage of providing the designer with fruitful information for EMC-oriented design.

In this framework, the EMC Community is rapidly moving towards stochastic modeling [1]–[4], in order to suitably cope with system complexity, which usually im-

plies randomness [5] and/or partial knowledge [6] of a number of the involved electrical and geometrical parameters. Hand-made cable assemblies, still employed as the common practice for implementing onboard interconnections, represent a problematic case, [5]. The effectiveness of deterministic modeling of signal transmission in these wiring structures is weakened by uncontrolled/random displacement of the wires in the cable cross-section, often leading to unacceptable over- or under-estimation of the actual susceptibility levels.

This is well exemplified by the test case considered in this work, where the radiated immunity of a random bundle of twisted-wire pairs (TWPs) mounted in a small satellite and subject to an internal source of interference, is investigated by measuring and predicting the noise induced in the cable terminations. Noise sensitivity to different bundle configurations is preliminary evidenced by measurement using an ad hoc setup, involving a full-scale mock-up of the AGILE scientific satellite, [7]. To this end, a suitably-fed monopole antenna is used to reproduce a harsh EM environment (characterized by nonuniform and highly resonant field) inside the metallic body of the satellite. Several hand-made assembled bundles are installed into the mock-up, and the common-mode (CM) and differential-mode (DM) noise voltages induced in the cable terminations are measured by a data-acquisition system.

Prediction of the induced noise levels is done by a statistical EMC model conceived as a trade-off between prediction accuracy and computational efficiency. Indeed, to reduce the computational burden required by repeated, full-wave simulations of the entire system, a single fullwave simulation of the satellite mock-up in the absence of the cable harness [8], [9] is combined with a statistical multiconductor transmission line (MTL) model of the random bundle, based on a previously developed description of field coupling to TWPs [9]–[11]. In the model, the cable is represented as the chain connection of uniform MTL sections [12] with cross-sections characterized by different positioning of the TWPs, which are allowed to randomly swap along the cable length. Computational efficiency of the model stems from the fact that MTL modeling of the involved bundle sections are derived from a single reference solution through suitable permutations of the involved matrices and vectors, and do not need to be re-evaluated section-by-section. This signif-

Manuscript received October 14, 2014.

Manuscript revised February 4, 2015.

[†]The authors are with the Department of Electronics, Information and Bioengineering, Politecnico di Milano, Milan, Italy.

^{††}The author is with European Space Research and Technology Centre (ESTEC) of the European Space Agency (ESA), Noordwijk, The Netherlands.

a) E-mail: flavia.grassi@polimi.it (Corresponding author)

b) E-mail: giordano.spadacini@polimi.it

c) E-mail: sergio.pignari@polimi.it

d) E-mail: filippo.marliani@esa.int

DOI: 10.1587/transcom.E98.B.1204

icantly speeds up the generation and subsequent simulation of different samples of the same random bundle, and allows fast prediction of the noise levels induced in the terminal units.

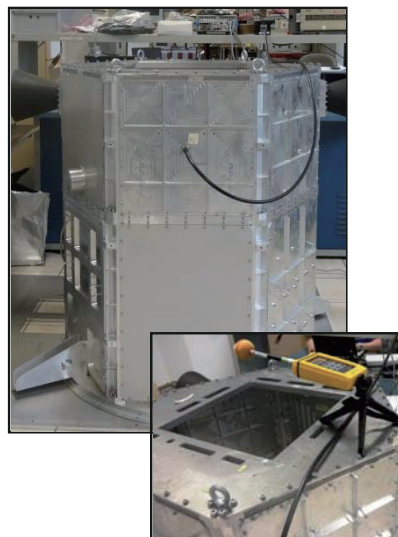
The rest of the paper is organized as follows. The test case under study is described in Sect. 2, and sensitivity to different bundle realizations is proved by repeated experimental measurements in Sect. 3. The proposed modeling strategy is described in Sect. 4. In Sect. 5, stochastic modeling of the random bundle is presented, and the obtained estimation of interference levels is compared versus measurement data. Finally, concluding remarks are drawn in Sect. 6.

2. Test-Case Under Study

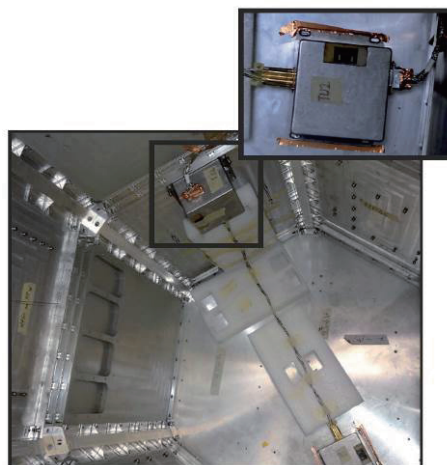
As a specific test-case of interest for the space sector, intra-system compatibility onboard a small satellite is here studied. In particular, measurement and prediction presented in the reminder of this work are obtained resorting to a full-scale mock-up of the AGILE satellite, which was sent into orbit in 2007 in the framework of an Italian scientific mission, [7]. Such a mock-up exactly reproduces the metallic chassis of the satellite (see Fig. 1), with the exception of the scientific payload and the solar-panel array, which are not of interest for the presented analysis. Mock-up base is hexagonal with side length ~ 40 cm and height ~ 120 cm. The whole structure does not present apertures, with the exception of the upper base, which is equipped with a large square window bordered by additional small holes, which — in the real satellite — are used to fasten the payload.

To assess susceptibility of hand-made random bundles of TWPs to radio frequency (RF) EM fields inside the satellite, the mock-up was equipped as follows.

Two terminal units [see Fig. 1(b)] were fastened to the lower base (lower terminal unit) and to one of the lateral panels (upper terminal unit) of the mock-up, and interconnected by the cable bundle under analysis. In this arrangement, the cable axis (with overall length ~ 900 mm) is kept at a constant distance, i.e., 50 mm, away from the nearest metallic surface by the use of non-conductive holders, and draws a bending angle of 90° between the horizontal and vertical straight sections. Each unit (see Fig. 2 for a principle drawing) is hosted inside a metallic box with side ~ 100 mm, and connected with the terminations of the cable bundle on one side (left side in Fig. 2), and with a wired link to the measurement system on the opposite side (right side in Fig. 2). In particular, since the bundle samples here considered are composed of six TWPs, six twinax connectors were soldered at the input of each metallic box. The inner circuitry is aimed at effective separation and measurement of the CM and DM noise induced by the external EM field at the terminations of each TWP in the bundle [6]. According to the circuit layout shown in Fig. 2, the separation of modal noise components is achieved by the use of six broadband center-tapped transformers, whereas twelve log-linear radio-frequency (RF) detectors are used to convert the ob-



(a)



(b)

Fig. 1 Pictures of the full-scale mock-up of the AGILE satellite during the experimental campaign: (a) outer, and (b) inner view.

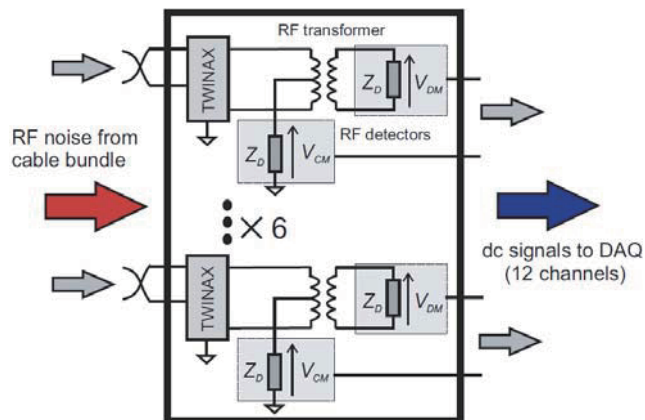


Fig. 2 Terminal units: Principle drawing of the inner circuitry. Input impedances seen from the terminals of each TWP looking towards the detectors are on the order of 100–200 Ω for the DM and of 30–70 Ω for the CM.

tained CM and DM voltages into dc signals. This prevents the RF noise possibly picked up by the wired connection (from the detectors to the measurement system) from corrupting the measurement data.

Finally, for RF field generation, a monopole antenna (with wire radius 0.5 mm and length 120 mm) was installed in the middle and orthogonal to one of the lateral panels, and fed from the outside by means of a N-type pass-through connector [upper picture in Fig. 1(a)].

3. Measurement

3.1 Field Generation and Data Acquisition

CM and DM noise voltages induced at the terminations of each TWP in the bundle were measured in the frequency range from 250 MHz to 1 GHz by feeding the monopole antenna with a constant forward-power level of 16 dBm. A principle drawing of the measurement and data-acquisition system is shown in Fig. 3. According to this block diagram, the system feeding the monopole antenna (upper part of the diagram) is synchronized with the system devoted to acquire and elaborate the noise levels picked-up at the terminal units (lower part of the diagram) by a customized software run by a computer. To provide a constant forward power level at the input of the monopole antenna, the forward power at the output of the feeding system (i.e., the RF generator and amplifier) is closed-loop monitored and kept constant by a directional coupler and a power meter. The dc signals coming from both the terminal units are collected by a data-acquisition (DAQ) board, and post-processed in order to retrieve the corresponding RF levels at the input pins of each terminal unit. To this end, a suitable algorithm was developed, which accounts for: (a) the input-output log-linear relationship of the RF detectors; (b) the stretches of twinax cables inside the boxes (see Fig. 2); and (c) the transfer function of the RF transformers. In particular, preliminary experimental characterization based on scattering-parameter measurement by a Vector Network Analyzer was used to derive the frequency-dependent characteristic parameters (i.e., slope and intercept, [13]) of the detectors and to retrieve the transfer functions relating modal voltages at the input and output ports of the RF transformers. Conversely, the twinax sections were modelled as lossless and balanced MTLs with DM and CM characteristic impedance $100\ \Omega$ and $30\ \Omega$, respectively, and propagation velocity $v = 0.75 v_0$, where v_0 is the speed of light in free-space (indeed, inside shielded cables/connectors, CM and DM propagation velocities can be assumed practically equal, since the medium surrounding the wires is almost homogeneous).

3.2 Measurement Results

To achieve a random wire arrangement, six different samples of the same bundle were hand-made assembled and installed into the satellite mock-up. Each sample is composed

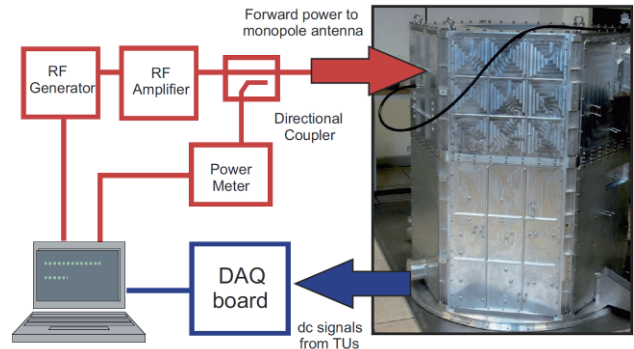


Fig. 3 Block diagram of the measurement and data acquisition system.

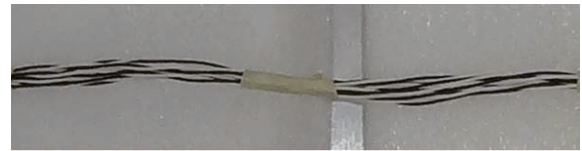


Fig. 4 Picture of one of the six hand-made bundle samples prepared for the test campaign and installed into the satellite mock-up.

by six AWG 24 pairs with overall length ~ 900 mm (an example of bundle sample is shown in Fig. 4.) Measurements were carried out for each bundle sample and yielded a collection of 36 CM and 36 DM-voltage frequency responses for each terminal unit. The CM and DM voltages measured at the upper terminal units and post-processed according to the algorithm described in the previous sub-section are plotted in Fig. 5, and reveal the large sensitivity of both modal noise components to different bundle configurations. Namely, in spite of the equal cable path, terminations, and impinging EM field, the TWPs in the bundle experience significantly different levels of CM and DM noise, with a spread spanning from 20 and 40 decibels.

4. Modeling Strategy

To retain system complexity (i.e., randomness related to bundle geometry), while avoiding the excessive computational burden required by repeated-run fullwave simulations of the system under analysis, the field-to-wire coupling problem is solved in two subsequent steps. First, the incident electric field generated by the monopole antenna is evaluated and sampled in different positions along the cable axis by a single fullwave simulation, involving an accurate 3D representation of the satellite mock-up. Second, the obtained electric-field samples are exploited in combination with a computationally-efficient stochastic model of the random bundle based on MTL theory, and accounting for random variations of TWPs positioning in the cable cross-section.

4.1 Computation of the Incident EM Field

According to the Agrawal model [8], interference due to the

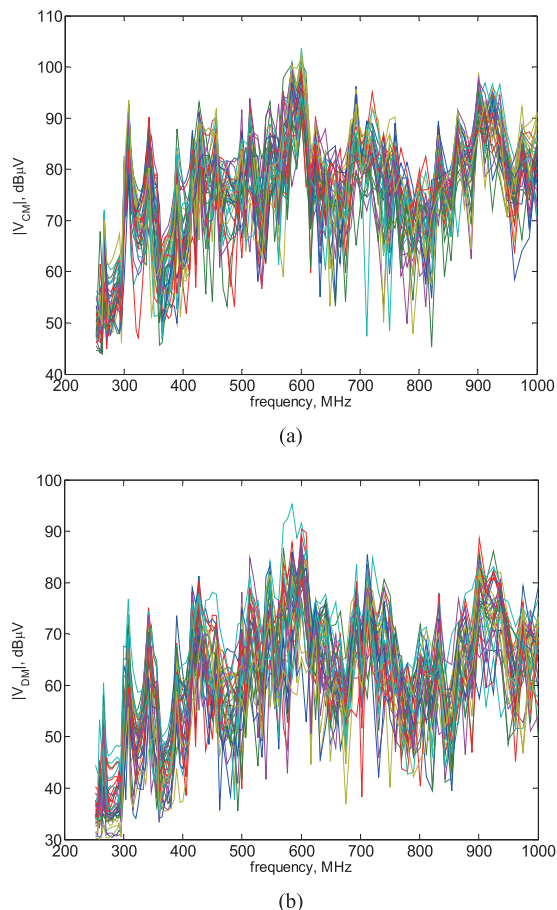


Fig. 5 Frequency response of the CM (a) and DM (b) voltages measured at the upper terminal unit.

incident EM field can be included into the MTL representation of the victim harness by (a) distributed voltage sources equal to the horizontal component of the electric field along the bundle axis, and (b) lumped voltage sources dependent on the vertical component of the electric field vector at line terminals. Consequently, computation of the incident electric field at the bundle position with the bundle removed [8], [9] is required, and involves EM simulation by fullwave numerical solvers.

To this end, the CAD model of the AGILE mock-up—equipped with the monopole antenna and terminal units—was imported in EMSS FEKO and simulated by the Method of Moments (MoM), [14]. The original CAD layout [see Fig. 6(a)] was preliminary simplified by removing details, such as screws and small holes, not significantly contributing to the overall field distribution in the frequency range up to 1 GHz. Additionally, instead of by a 3D model of the cable bundle, the two terminal units were interconnected by a virtual line coincident with the cable axis [line labelled as “cable-path” in Fig. 6(b)], along which the horizontal and vertical electric-field components (as required for subsequent MTL modeling) were sampled.

For simulation, the structure was excited by a monopole antenna fed according to the forward power levels

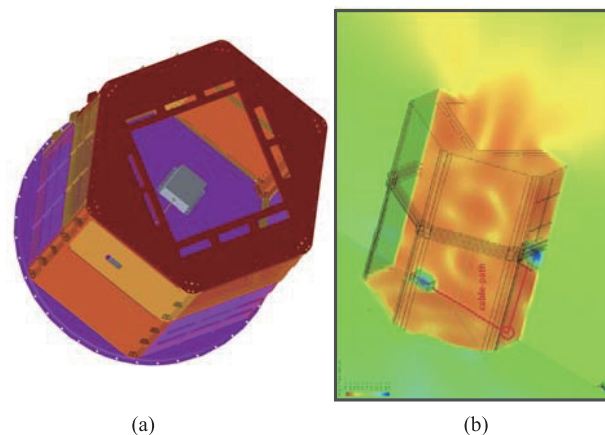


Fig. 6 Computation of the incident EM field: (a) CAD model of the AGILE mock-up imported and (b) simulated in the 3D numerical solver FEKO, [14].

in Sect. 3, and simply implemented in the simulation environment by means of a thin wire. Near-field computation was carried out for 100 frequency points in the frequency range from 250 MHz up to 1 GHz and required about 120 hours of run-time and 30 GByte of memory. As an example of simulation results, the color map of the electric-field strength obtained at 1 GHz in the plane of the cable path is shown in Fig. 6(b).

5. Stochastic Modeling of the Random Bundle

To account for random TWPs displacement in the cable cross-section, while retaining computational efficiency, the following simplifying assumptions are introduced.

First, nonuniformity associated with wire-twisting inside each TWP is disregarded. Accordingly, the two wires in each TWP are modelled as a uniform balanced structure above ground, characterized by per unit length (p.u.l.) inductance and capacitance parameters averaged over the twist-pitch length [9], [11].

Second, the presence of wire coating is neglected, since it has been proved by previous analyses that such an approximation does not significantly impact on the prediction of CM voltages at the cable ends [9].

Third, the cable is subdivided into N_S sections of equal length \mathcal{L} , along which the relative position of each TWP in the cable cross-section can be considered as nearly constant. This subdivision depends on the specific manufacture of the cable bundle under analysis and, besides being directly inferred by cable inspection, does not introduce any frequency limitation to model validity.

Based on the above-listed assumptions, the cable bundle is modelled as the cascade connection of N_S uniform MTL sections, differing each other for TWP positioning inside a reference cross-section.

5.1 Field-To-Wire Coupling Model

The main steps at the basis of the solution process are

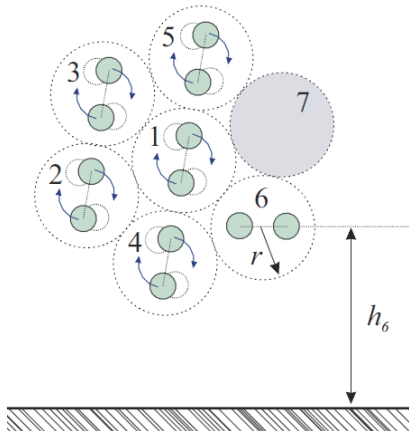


Fig. 7 Reference cross-section associated with the random bundle under analysis.

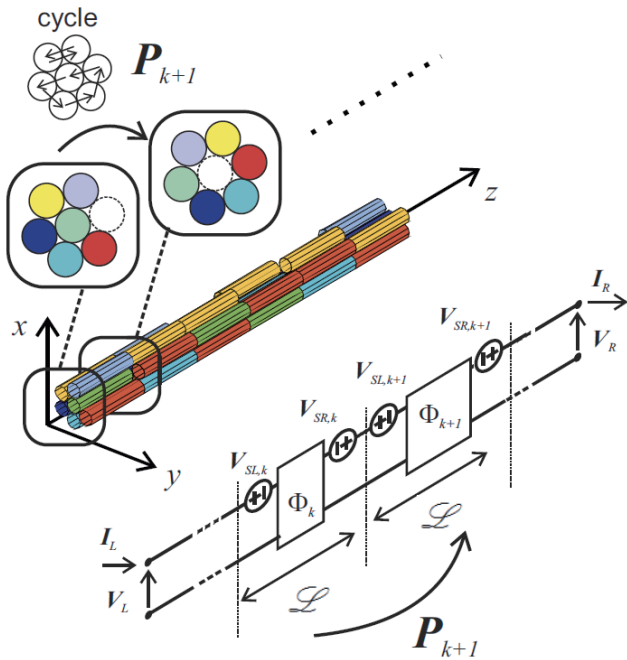


Fig. 8 Principle drawing of the solution process. Each sample of random bundle is modelled as the cascade connection of uniform MTL sections, whose cross-sections differ for TWP positioning. This is done by letting the TWPs randomly swapping their position section-by-section (i.e., by following a so-called cycle) with minimum-distance interchanges.

schematically summarized in Fig. 7 and Fig. 8. The starting point is the introduction of a suitable reference cross-section. In such a cross-section, each TWP is represented through a circle with center in the TWP axis and radius r , which denotes the overall dimension of each wire pair, including the space occupied by wire coating (despite the presence of any dielectric material is here neglected, [9]). In this representation, nonuniformity associated with wire twisting is disregarded, and two wires in the TWP are modelled as a perfectly-balanced pair, characterized by averaged p.u.l. parameters over the twist-pitch, [9], [11]. In particu-

lar, for the specific cable bundle under analysis, a reference cross-section with seven rooms is selected to approximate a compact, pseudo-circular shape, as shown in Fig. 7.

Given the reference cross-section (and an initial TWP numbering), the MTL model of the corresponding bundle section is derived, which includes: (a) a passive 24-port network, representative for propagation effects along the bundle section, and (b) twenty-four induced voltage sources (twelve on each side of the passive network), accounting for the effects due to the interfering EM field.

In the following, this bundle section will be denoted as “reference section”, since MTL modeling of the other sections will be derived starting from this reference solution by permutations of rows and columns in the involved matrices and vectors.

Regarding the passive part of the model, the analytical expression of the involved 24×24 chain-parameter matrix Φ can be cast as:

$$\Phi = \begin{bmatrix} \cos(\beta_0 \mathcal{L}) \mathbf{1}_{12} & -jv_0 \sin(\beta_0 \mathcal{L}) \mathbf{L} \\ -jv_0^{-1} \sin(\beta_0 \mathcal{L}) \mathbf{L}^{-1} & \cos(\beta_0 \mathcal{L}) \mathbf{1}_{12} \end{bmatrix} \quad (1)$$

where $\beta_0 = \omega/v_0$ is the propagation constant, \mathcal{L} is the length of each bundle section, and $\mathbf{1}_{12}$ is the 12×12 identity matrix. Finally, \mathbf{L} denotes the 12×12 p.u.l. inductance matrix associated with the reference cross-section, whose entries can be efficiently evaluated by the approximate analytical expressions—not reported here for the sake of brevity—in [9].

Concerning the active part of the model, equal voltage sources are assumed to act on the two wires belonging to the same TWP, in line with the assumption of balanced TWPs. Accordingly, for each TWP in the bundle the pairs of open-end voltage sources by each side of the passive block are evaluated by numerical approximation of the following closed-form integrals, [9], [11]:

$$V_{SL,j} = \int_0^{\mathcal{L}} \frac{\sin[\beta_0(z-\mathcal{L})]}{\sin(\beta_0 \mathcal{L})} E_z(h_j, 0, z) dz - \int_0^{h_j} E_x(x, 0, 0) dx \quad (2)$$

$$V_{SR,j} = \int_0^{\mathcal{L}} \frac{\sin(\beta_0 z)}{\sin(\beta_0 \mathcal{L})} E_z(h_j, 0, z) dz - \int_0^{h_j} E_x(x, 0, \mathcal{L}) dx \quad (3)$$

where $j = 1, 2, \dots, 6$ denotes the j -th TWP in the reference cross-section, h_j is the height of the j -th TWP axis, and E_z , E_x are the longitudinal and vertical electric-field components computed by EM simulation and sampled along the cable axis.

It's worth noting here that setting equal voltage sources on both the two wires in the same TWP implies assuming that DM noise components on average cancel out within the twisted-line. Accordingly, only distributed CM excitation of the wires is considered here, as it was proved to be dominant over DM excitation in the frequency range of interest for the presented analysis, [11]. In line with this assumption, the non-null DM voltages picked-up at the cable ends are only to be ascribed to CM-to-DM conversion due to the imbalance introduced by the terminal networks [15]–[18],

and can be computed afterwards as in [15].

5.2 Generation and Modeling of Bundle Samples

To account for random displacement of the TWPs along the bundle axis, TWP positioning within the reference cross-section is allowed to vary section-by-section by minimum-distance interchanges, so to ensure smooth and physically sound transitions. To this end, a suitable algorithm based on the Theory of Graphs [19] is developed, which provides all possible sets of TWP interchanges (in the following denoted as cycles) within the reference cross-section. For the specific cross-section here considered, this procedure yields more than two hundred possible cycles, which can be preliminary stored, and used to generate several samples of the same cable bundle. To this end, a sub-set of N_S cycles is randomly selected for each sample (according to a uniform-discrete probability distribution), and applied to each bundle section (starting from the reference cross-section) to generate TWPs arrangement in the subsequent section (see Fig. 8).

MTL modeling of the obtained cable sections is then efficiently evaluated starting from the chain-parameter matrix and induced sources of the reference section in (1)–(3) by associating with every cycle a permutation matrix \mathbf{P}_k , whose 2×2 sub-matrices are all zero except for sub-matrix

$$\mathbf{P}_{ij} = \mathbf{1}_2 \text{ if TWP } i \text{ moves to position } j \quad (4)$$

where $i, j = 1, 2, \dots, 6$ and $\mathbf{1}_2$ denotes the 2×2 identity matrix. As an example, the permutation matrix associated with the cycle exemplified in Fig. 8 (and derived according to TWP numbering in the reference cross-section shown in Fig. 7) takes the form

$$\mathbf{P}_{k+1} = \begin{bmatrix} \mathbf{0}_2 & \mathbf{1}_2 & \mathbf{0}_2 & \mathbf{0}_2 & \mathbf{0}_2 & \mathbf{0}_2 & \mathbf{0}_2 \\ \mathbf{0}_2 & \mathbf{0}_2 & \mathbf{0}_2 & \mathbf{1}_2 & \mathbf{0}_2 & \mathbf{0}_2 & \mathbf{0}_2 \\ \mathbf{0}_2 & \mathbf{0}_2 & \mathbf{0}_2 & \mathbf{0}_2 & \mathbf{1}_2 & \mathbf{0}_2 & \mathbf{0}_2 \\ \mathbf{0}_2 & \mathbf{0}_2 & \mathbf{0}_2 & \mathbf{0}_2 & \mathbf{0}_2 & \mathbf{1}_2 & \mathbf{0}_2 \\ \mathbf{0}_2 & \mathbf{0}_2 & \mathbf{1}_2 & \mathbf{0}_2 & \mathbf{0}_2 & \mathbf{0}_2 & \mathbf{0}_2 \\ \mathbf{0}_2 & \mathbf{0}_2 & \mathbf{0}_2 & \mathbf{0}_2 & \mathbf{0}_2 & \mathbf{0}_2 & \mathbf{1}_2 \\ \mathbf{1}_2 & \mathbf{0}_2 & \mathbf{0}_2 & \mathbf{0}_2 & \mathbf{0}_2 & \mathbf{0}_2 & \mathbf{0}_2 \end{bmatrix} \quad (5)$$

where $\mathbf{0}_2$ denotes the 2×2 zero matrix.

Such a linear transformation is iteratively applied to the chain-parameter matrix and induced source vector of each cable section [starting from those of the reference section in (1)–(3)] to derive the MTL model of the adjacent section in the bundle. In this way, moving from section $k-1$ to section k only requires permutations in the rows and columns in the involved matrices and vectors, [20].

5.3 Prediction of Interference Levels

To predict modal noise voltages induced at the terminations of the random bundle under analysis, the cable was subdivided into $N_S = 8$ MTL sections (this choice being in line with the specific hand-made assembly procedure used to

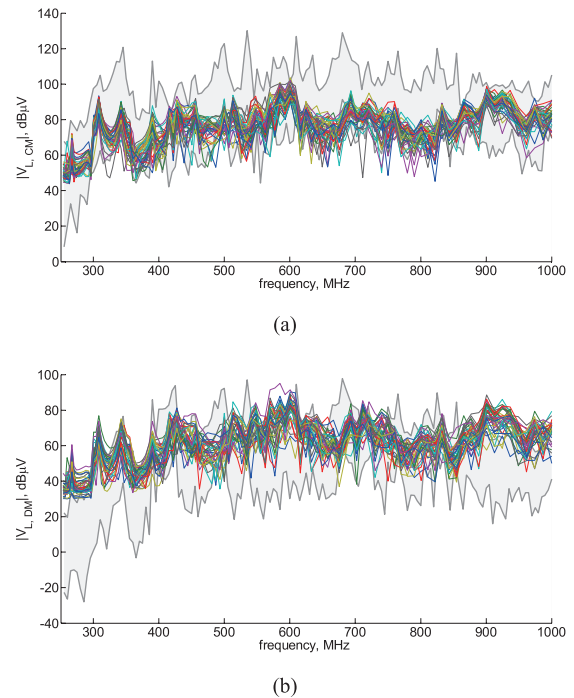


Fig. 9 CM (a) and DM (b) voltages at the upper terminal unit (overall bundle length ~ 900 mm): comparison between the susceptibility interval provided by the proposed model (grey area) and measurement data (colored curves).

prepare the six bundle samples in Sect. 3), and one hundred bundle samples were generated by randomly combining the available cycles. For each sample, line solution was then accomplished by cascade-connecting the MTL models of each section (as in Fig. 8), and by combining the obtained 24-port representation with the port constraints enforced by the terminal units.

The whole simulation lasted about 1 hour running on a Pentium IV computer equipped with 24 Gbyte RAM. Outcome of the simulation is obtained in the form of an interval of susceptibility levels (bounded by minimum and maximum CM and DM voltages), the measured CM and DM voltages at the terminal units are reasonably expected to fall in. The obtained predictions are compared versus measurement data in Fig. 9 and Fig. 10, where the “susceptibility interval” provided by simulation is shown in grey, and measurement data are plotted by colored curves. On the whole, the predicted intervals exhibit a satisfactory coverage of the measurement data in the whole frequency range up to 1 GHz, with the peaks characterizing the measured frequency responses remarkably reproduced by simulations. Over-estimation of the spread (amplitude of susceptibility intervals) obtained by measurement can be explained considering that the statistical relevance of the simulation and experimental data sets is not directly comparable. Indeed, while the former set of data is composed of 600 frequency responses for each modal voltage, the latter comprises 36 samples only.

Possible underestimation of the DM noise is due to the

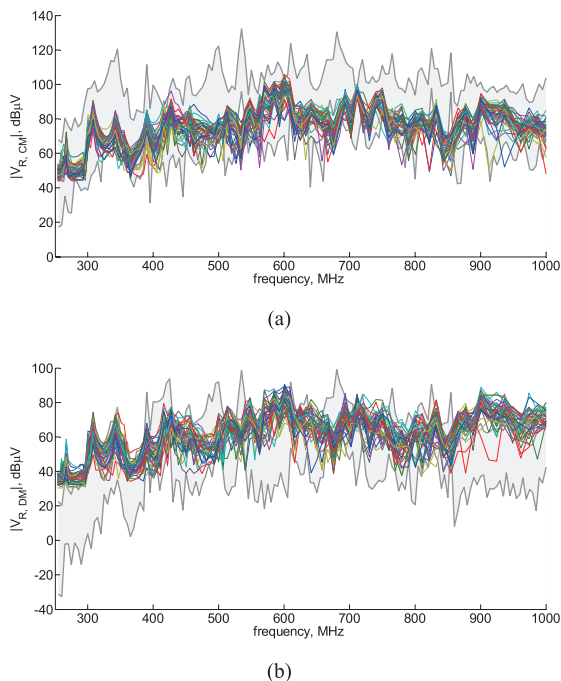


Fig. 10 CM (a) and DM (b) voltages at the lower terminal unit (overall bundle length ~ 900 mm): comparison between the susceptibility interval provided by the proposed model (grey area) and measurement data (colored curves).

fact that in the proposed simplified model the DM is not directly excited by the EM field, but it is only to be ascribed to CM-to-DM conversion due to imbalance affecting the terminal networks, [15], [16]. However, in the high frequency range the contribution due to pure DM excitation becomes no longer negligible [9], thus possibly leading to noise levels higher than those predicted by simulation. Besides, the DM is expected to be more sensitive than the CM to the simplifying assumption of neglecting the presence of any dielectric material. However, this assumption is here introduced as a trade-off between prediction accuracy and computational efficiency. Special reference also needs to be made to the low frequency interval from 250 to 300 MHz, where underestimation is due to the fact that the predicted levels of DM voltages are well below the sensitivity of the measurement system (about $30 \text{ dB}\mu\text{V}$).

6. Conclusion

In this work, a simplified and computationally-efficient fullwave-MTL model providing fast prediction of the CM and DM voltages induced at the terminations of a random TWP bundle onboard a small satellite was presented.

Unlike previous works on the subject [9], [11], that were developed and validated with reference to canonical EM environments (i.e., uniform plane-wave field) and well-controlled wiring harnesses, we introduced a real test case, where uncertainty and partial knowledge of the involved setup parameters are allowed for. Namely, complexity of the nonuniform and highly-resonating EM field inside the

satellite metallic body is accounted for by means of a single fullwave simulation. Randomness of the cable geometry is represented by generation and simulation of several bundle samples, characterized by random displacement of the TWPs along the cable axis. Prediction reliability was confirmed by comparison to measurement data. The results stress the need for a stochastic instead of a deterministic modeling approach, in order to account for the significant spread of the frequency response of induced voltages.

References

- [1] C. Jullien, P. Besnier, M. Dunand, and I. Junqua, "Advanced modeling of crosstalk between an unshielded twisted pair cable and an unshielded wire above a ground plane," *IEEE Trans. Electromagn. Compat.*, vol.55, no.1, pp.183–194, Feb. 2013.
- [2] F. Paladian, P. Bonnet, and S. Lallechere, "Modeling complex systems for EMC applications by considering uncertainties," *Proc. XXXth U.R.S.I.G.A.*, pp.1–4, Istanbul, Turkey, Aug. 2011.
- [3] M. Wu, D.G. Beetner, T.H. Hubing, H. Ke, and S. Sun, "Statistical prediction of "Reasonable worst-case" crosstalk in cable bundles," *IEEE Trans. Electromagn. Compat.*, vol.51, no.3, pp.842–851, Aug. 2009.
- [4] G. Spadacini and S.A. Pignari, "Radiated susceptibility of a twisted-wire pair illuminated by a random plane-wave spectrum," *IEICE Trans. Commun.*, vol.E93-B, no.7, pp.1781–1787, July 2010.
- [5] S. Sun, G. Liu, J.L. Drewniak, and D.J. Pommerenke, "Hand-assembled cable bundle modeling for crosstalk and common-mode radiation prediction," *IEEE Trans. Electromagn. Compat.*, vol.49, no.3, pp.708–718, Aug. 2007.
- [6] F. Grassi, G. Spadacini, S.A. Pignari, and F. Marliani, "Sensitivity to setup configuration of the response of differential lines driven by an external field," *Proc. 2014 IEEE Int. Symp. on Electromagn. Compat.*, pp.852–855, Tokyo, Japan, May 2014.
- [7] G. Spadacini, F. Grassi, F. Marliani, and S.A. Pignari, "Transmission-line model for field-to-wire coupling in bundles of twisted-wire pairs above ground," *IEEE Trans. Electromagn. Compat.*, vol.56, no.6, pp.1682–1690, Tokyo, Japan, May 2014.
- [8] M. Tavani, G. Barbiellini, A. Argan, A. Bulgarelli, P. Caraveo, A. Chen, V. Cocco, E. Costa, G. De Paris, E.D. Monte, G.D. Cocco, I. Donnarumma, M. Feroci, M. Fiorini, T. Froyland, F. Fuschino, M. Galli, F. Gianotti, A. Giuliani, Y. Evangelista, C. Labanti, I. Lapshov, F. Lazzarotto, P. Lipari, F. Longo, M. Marisaldi, M. Mastropietro, F. Mauri, S. Mereghetti, E. Morelli, A. Morselli, L. Pacciani, A. Pellizzoni, F. Perotti, P. Picozza, C. Pontoni, G. Porrovecchio, M. Prest, G. Pucella, M. Rapisarda, E. Rossi, A. Rubini, P. Soffitta, M. Trifoglio, A. Trois, E. Vallazza, S. Vercellone, A. Zambra, D. Zanello, P. Giommi, A. Antonelli, and C. Pittori, "The AGILE space mission," *Nuclear Instruments and Methods in Physics Research Sect. A: Accelerators, Spectrometers, Detectors and Associated Equipment*, vol.588, no.1-2, pp.52–62, April 2008.
- [9] A.K. Agrawal, H.J. Price, and S.H. Gurbaxani, "Transient response of multiconductor transmission lines excited by a nonuniform electromagnetic field," *IEEE Trans. Electromagn. Compat.*, vol.EMC-22, no.2, pp.119–129, May 1980.
- [10] G. Spadacini, F. Grassi, F. Marliani, and S.A. Pignari, "Transmission-line model for field-to-wire coupling in bundles of twisted-wire pairs above ground," *IEEE Trans. Electromagn. Compat.*, Vol.56, no.6, pp.1682–1690, Dec. 2014.
- [11] C.D. Taylor and J.P. Castillo, "On the response of a terminated twisted-wire cable excited by a plane-wave electromagnetic field," *IEEE Trans. Electromagn. Compat.*, vol.EMC-22, no.1, pp.16–19, Feb. 1980.
- [12] S.A. Pignari and G. Spadacini, "Plane-wave coupling to a twisted-wire pair above ground," *IEEE Trans. Electromagn. Compat.*,

- vol.53, no.2, pp.508–523, May 2011.
- [12] M. Omid, Y. Kami, and M. Hayakawa, “Field coupling to nonuniform and uniform transmission lines,” *IEEE Trans. Electromagn. Compat.*, vol.39, no.3, pp.201–211, Aug. 1997.
- [13] Linear Technology, LT5537-Wide dynamic range RF/IF log detectors, Application Note. Available online: <http://cds.linear.com/docs/en/datasheet/5537fa.pdf>
- [14] FEKO Suite 6.3 User’s Manual (Oct. 2013), © EM Software and Systems, Stellenbosch, South Africa, www.feko.info
- [15] F. Grassi, G. Spadacini, and S.A. Pignari, “The concept of weak imbalance and its role in the emissions and immunity of differential lines,” *IEEE Trans. Electromagn. Compat.*, vol.55, no.6, pp.1346–1349, Dec. 2013.
- [16] A. Sugiura and Y. Kami, “Generation and propagation of common-mode currents in a balanced two-conductor line,” *IEEE Trans. Electromagn. Compat.*, vol.54, no.2, pp.466–473, April 2012.
- [17] F. Grassi and S.A. Pignari, “Bulk current injection in twisted wire pairs with not perfectly balanced terminations,” *IEEE Trans. Electromagn. Compat.*, vol.55, no.6, pp.1293–1301, Dec. 2013.
- [18] F. Grassi, G. Spadacini, and S.A. Pignari, “SPICE behavioral modeling of RF current injection in wire bundles,” *IEEE Trans. Commun.*, vol.E97-B, no.2, pp.424–431, Feb. 2014.
- [19] G. Danielson, “On finding the simple paths and circuits in a graph,” *IEEE Trans. Circuit Theory*, vol.15, no.3, pp.294–295, Sept. 1968.
- [20] D. Bellan and S.A. Pignari, “Efficient estimation of crosstalk statistics in random wire bundles with lacing cords,” *IEEE Trans. Electromagn. Compat.*, vol.53, no.1, pp.209–218, Feb. 2011.



Flavia Grassi received the Laurea and Ph.D. degrees in electrical engineering from the Politecnico di Milano, Italy, in 2002 and 2006, respectively, where she is currently an Assistant Professor with the Department of Electronics, Information and Bioengineering. From 2008 to 2009, she was with the European Space Agency (ESA), The Netherlands. Her research interests are focused on the characterization of measurement setups for electromagnetic compatibility testing (aerospace and automotive sectors), and

applications of the powerline communications (PLC) technology on ac and dc lines.



Giordano Spadacini received the Laurea (M.S.) and Ph.D. degrees in electrical engineering from the Politecnico di Milano, Milan, Italy, in 2001 and 2005, respectively. Since 2007 he has been an Assistant Professor at the Politecnico di Milano, Department of Electronics, Information and Bioengineering. His research interests include distributed-parameter circuit modeling, statistical models for the characterization of interference effects, and EMC in railway and aerospace systems. Dr. Spadacini

received the IEEE EMC Transactions Prize Paper Award for the best paper published in 2004.



Sergio A. Pignari received the Laurea and Ph.D. degrees in electronic engineering from the Politecnico di Torino, Turin, Italy, in 1988 and 1993, respectively. From 1991 to 1998, he was an Assistant Professor with the Department of Electronics, Politecnico di Torino, Turin, Italy. In 1998, he joined Politecnico di Milano, Milan, Italy, where he is currently a Full Professor of Circuit Theory and Electromagnetic Compatibility (EMC) with the EMC Group, at the Department of Electronics, Information, and Bio-

engineering. He is the author or coauthor of more than 130 papers published in international journals and conference proceedings. His current research interests include characterization of interference effects, distributed parameter circuit modeling, statistical techniques for EMC, and experimental procedures and setups for EMC testing. Dr. Pignari was the recipient of the IEEE EMC Society 2004 Transactions Prize Paper Award. He is currently an Associate Editor of the IEEE Transactions on Electromagnetic Compatibility and the IEEE EMC Society Chapter Coordinator.



Filippo Marliani received the Laurea degree in electronic engineering from the University of Florence, Italy, in 1997. From 1998 to 1999, he was with the Electromagnetics Group, MIT, Cambridge, MA. Since November 1999, he has been with the Electromagnetics and Space Environments Division, European Space Agency, Noordwijk, The Netherlands, where, since 2007, he has been the Head of the Electromagnetic Compatibility Section. His current research interests include theoretical and numerical

electromagnetics for EMC, measurement procedures for unit- and system-level EMC testing of space systems.